# 3-Chloromethylpyridyl bipyridine *fac*-tricarbonyl rhenium: a thiol-reactive luminophore for fluorescence microscopy accumulates in mitochondria†‡

**Angelo J. Amoroso,[a] Richard J. Arthur,[a] Michael P. Coogan,*[a] Jonathan B. Court,[b] Vanesa Fernández-Moreira,[a] Anthony J. Hayes,[c] David Lloyd,[b] Coralie Millet[b] and Simon J. A. Pope[a]**

*Received (in Montpellier, France) 8th February 2008, Accepted 18th April 2008*
*First published as an Advance Article on the web 23rd May 2008*
**DOI: 10.1039/b802215a**



**The 3-chloromethylpyridyl bipyridine *fac* tricarbonyl rhenium cation is a thiol-reactive luminescent agent with a long luminescence lifetime and large Stokes shift that is demonstrated by co-localisation studies to accumulate in mitochondria. This represents the first application of a $^3$MLCT luminescent agent for the specific targeting of a biological entity in imaging.**

Mitochondria, named from the Greek μιτος (thread) and κουδριον (grain), are believed to have their origin in a symbiotic relationship between early eukaryotes and archaic bacteria that were capable of performing roles unavailable to the host cells.[1a,b] Mitochondria generate most of a cell's energy by ATP synthesis, and have many other important roles in signalling, differentiation, cell division cycles and cell death.[1c,d] As such, mitochondria are an important target for biological investigation, and a wide variety of probes for their imaging have been developed. One of the most important classes of mitochondrial probe are the MitoTracker™ probes,[2] membrane permeable thiol reactive dyes containing a chloromethyl group that specifically stain mitochondria. Rhenium tricarbonyl bisimine complexes are well know as triplet metal-to-ligand charge transfer ($^3$MLCT) luminescent materials with useful photophysical properties, including large Stokes shifts, long lifetimes and good quantum yields,[3] that have long been postulated but only recently demonstrated[4] to have applications in biological imaging as fluorochromes in fluorescence microscopy. These three advantages allow easy differentiation of their emission from interfering autofluorescence.

A rhenium complex functionalised with a chloromethyl unit thus has the potential to provide a thiol-reactive, possibly mitochondria-selective, probe with a long lifetime and a large Stokes shift, with clear potential for biological imaging. There have been previous reports[5] of rhenium and ruthenium bisimine complexes that are either thiol reactive or contain other species, which could localise due to biological interactions. All have long lifetimes and large Stokes shifts, making them attractive candidates for biological imaging applications. A rhenium quinoline complex[5b] has previously been bioconjugated to a peptide, and its localisation has been shown by fluorescence microscopy to be identical to that of a fluorescein-tagged peptide.

Following previous work,[4a] in which lipophilicising units were incorporated into the axial pyridine of these rhenium complexes, the *fac*-3-chloromethylpyridine rhenium tricarbonyl bipyridyl complex (**1**) was chosen as a representative chloromethyl rhenium fluorophore to study.

Traditional routes[3] to rhenium tricarbonyl bisimines involve the reaction of a bisimine (*e.g.* bipy, phen) with chlororhenium pentacarbonyl, followed by activation of the resultant tricarbonyl chlorobisimine rhenium species, **2**, by chloride abstraction and finally substitution with a ligand (typically phosphine or pyridine) to give the cationic complexes that have the most useful photophysics. Routes to chloromethylated species are typically based around either the incorporation of a chloromethyl group into a prefabricated component of the molecule or by the chlorination of an alcohol. As conditions for the chlorination of alcohols are often harsh, incorporating the pre-existing chloromethyl group of 3-chloromethylpyridine was chosen. However, treatment of the activated intermediate *fac*-$[Re(CO)_3(bpy)(MeCN)][BF_4]$ (**3**) with 3-chloromethylpyridine hydrochloride in the presence of base (triethylamine) gave not the pyridine complex, but instead the precursor material *fac*-$[Re(CO)_3(bpy)Cl][BF_4]$ (**2**). Inclusion of silver tetrafluoroborate in the reaction mixture in an attempt to precipitate the chloride, and thus prevent it from taking part in the reaction, was unsuccessful, and again chloro complex **2** was recovered. An attempt to provide a chloride-free chloromethyl pyridine by treating the hydrochloride salt with silver tetrafluoroborate in a precipitative salt metathesis was again unsuccessful, with a very slow reaction of the [Py-3-$CH_2Cl$]·$HBF_4$/triethylamine system with **3** giving a very low yield of

[a] *Department of Chemistry, Cardiff University, Cardiff, Wales, UK CF10 3AT. E-mail: cooganmp@cf.ac.uk; Fax: +44 (0)2920 874030; Tel: +44 (0)2920 874066*
[b] *Cardiff School of Biosciences, Main Building, Museum Avenue, Cardiff, Wales, UK CF10 3TL*
[c] *Confocal Microscopy Unit, Cardiff School of Biosciences, Life Sciences Building, Cardiff, Wales, UK CF10 3US*

† Electronic supplementary information (ESI) available: Co-localisation scatter plots. See DOI: 10.1039/b802215a

‡ Crystallographic data for **1**: $C_{19}H_{14}ClF_6N_3O_3PRe$, monoclinic, $P2_1/c$, $a$ = 13.7391(4), $b$ = 11.5590(4), $c$ = 14.6082(5) Å, $\beta$ = 100.743(2)°, $Z$ = 4, $T$ = 150 K, $\mu$ = 5.476 mm$^{-1}$, $\lambda$ = 0.71069 Å (Mo-$K_\alpha$), $F(000)$ = 1268, 2.96 < $\theta$ < 27.45, 5171 reflections, 3737 unique [$R_{int}$ = 0.1529], $R1$ = 0.0503, w$R2$ = 0.1094 [$I > 2\sigma(I)$], $R1$ = 0.0798, w$R2$ = 0.1219 (all data). CCDC 685598. For crystallographic data in CIF or other electronic format, see DOI: 10.1039/b802215a.

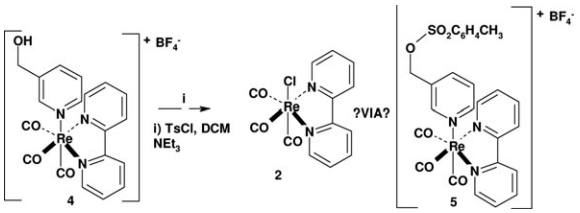


**Scheme 1** Attempted synthesis of **1**.

**2**. The chloride ion source for the production of **2** must be by displacement of chloride from the chloromethyl group, and it is surprising that this is faster than substitution of the axial acetonitrile of **3**. Given the difficulty of converting **3** to **2**, an alternative approach was attempted *via* tosylation of the analogous hydroxymethylpyridine complex $[Re(CO)_3(bpy)(3\text{-}Py\text{-}CH_2OH)][BF_4]$ (**4**). However, a reaction with tosyl chloride gave not a 3-tosyloxymethylpyridine complex but, again, chloro complex **2** (Scheme 1). This entirely unexpected result can only be rationalised in terms of an activation of the pyridine ligand towards displacement during the reaction with tosyl chloride, as the starting material is stable towards solutions containing chloride (a concerted tosylation–substitution is unlikely for a 3-hydroxymethylpyridine ligand). Finally, following a recent report[6] on the bromination of a similar system with thionyl bromide, the hydroxy–chloride conversion was successfully realised with thionyl chloride in DCM in 78% yield, after aqueous work-up and precipitation of the product as a hexafluorophosphate salt (Scheme 2).

In order to determine that the required complex had finally been synthesised, crystals that were suitable for X-ray analysis were grown by slow evaporation of a chloroform solution.‡ The structure of this species showed a *fac*-geometry of the three carbonyl ligands, bipyridine describing the equatorial plane and an axial chloromethylpyridine ligand completing the octahedral geometry (Fig. 1), with two pairs of mutual Cl–C close contacts (3.333 Å) between the chlorines of one complex and the carbonyl carbons of an adjacent complex (Fig. 2).

Chloromethyl complex **1** showed the typical photophysical properties of a cationic rhenium tricarbonyl bisimine;[1] excitation at $\lambda_{max}$ 364 nm, emission at $\lambda_{max}$ 551 nm and a fluorescence lifetime of $\tau$ = 131 ns. Having synthesised a chloromethylpyridine-substituted rhenium complex with a (reasonably) long fluorescence lifetime and a large Stokes shift, a variety of reactions with biologically-relevant potential nucleophiles were then undertaken to see whether the desired thiol specificity had been replicated. Complex **1** showed no reactivity with the amine groups of simple amino acids (or their esters) under mild, physiologically-relevant conditions, or towards the *N*-terminus of simple peptides. In a reaction

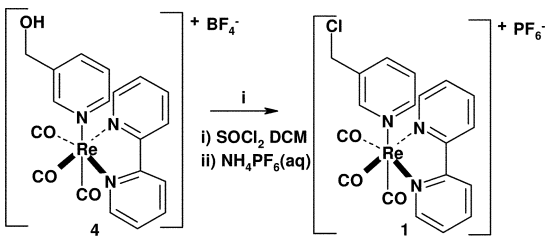


**Scheme 2** Synthesis of **1**.

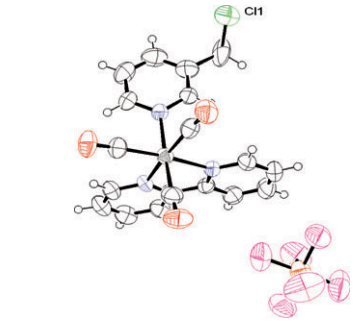


**Fig. 1** ORTEP representation of **1** (50% probabilities).

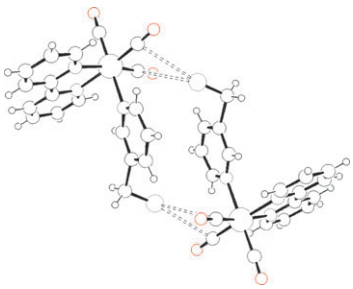

**Fig. 2** Close contacts in **1**.

with the mixed *N*,*S*-nucleophile cysteine methyl ester, exclusive *S*-alkylation was observed (Scheme 3), as demonstrated by the typical *S*-methylene shift of the 3-picolyl group in the $^{13}C$ NMR spectrum ($\delta$ 35.2), to give **6** in good yield (65%). In order to demonstrate reactivity with more complex biologically-relevant thiols, chloromethyl complex **1** was treated with reduced glutathione (GSH) in a methanol–water mixture at pH 9 (Scheme 4). The formation of a glutathione–rhenium conjugate, **7**, was indicated by the formation of a water soluble fluorescent complex, which was separated from unreacted **1** by evaporation to dryness, dissolution in water and filtration, before final purification by ion exchange chromatography (Amberlite IR120 resin, $NH_4^+$ form). Its structure was confirmed by HRMS. No reaction of **1** with water was observed, and it appeared to be hydrolytically stable under mild conditions for many hours.

The thiol adducts **6** and **7** showed the typical photophysical properties of a cationic rhenium tricarbonyl bisimine;[1] excitation at $\lambda_{max}$ **6** 360 nm and **7** 361 nm, emission at $\lambda_{max}$ **6** 550 nm, **7** 551 nm, and lifetimes of $\tau$ = **6** 122 ns, **7** 116 ns. The photophysical properties of the glutathione adduct **7** were particularly relevant as it is likely that this would be a major species produced from **1** in a mitochondrion.

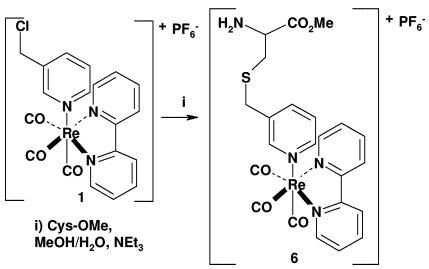


**Scheme 3** Reaction of **1** with cysteine.

 

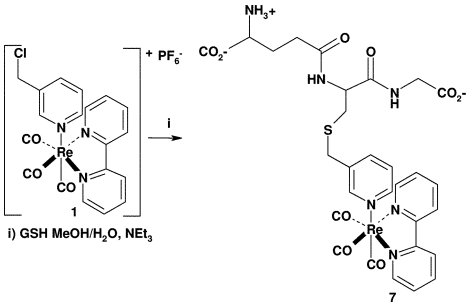


**Scheme 4** Reaction of **1** with glutathione.

With confirmation that **1** represents a potentially useful thiol-reactive luminescent dye, imaging experiments in *Saccharomyces Cerevisiae* IFO 0233 (yeast) cells were carried out, as yeast is a well characterised organism and the sites of localisation of the rhenium dyes might be identifiable with reference to the literature. Yeast cells were incubated in standard growth media after treatment with a DMSO solution of **1**, then fixed and examined by confocal microscopy. While the dye was clearly accumulated in a proportion of the cells, the general level of uptake was poor (Fig. 3(a)), but interestingly it appeared that the cells which had incorporated the fluorophore were in the process of budding (Fig. 3(b) and (c)). While a dye which is only taken up by cells at a certain stage of the life cycle is possibly of limited use it was interesting to note that in cells which had taken up **1** at low levels, localisation (Fig. 3(d)) had occurred in specific organelles, which are likely to be mitochondria, given the precedent for the localisation of cationic thiol reactive dyes.

Yeast cells are unlike mammalian cells in that they possess a rigid cell wall[7] that may slow or prevent the permeation of **1**, and thus further studies were undertaken using cultured mammalian cells. Human mammary adenocarcinoma cells (MCF-7)[8] were incubated with **1**, and the uptake and localisation were again studied by confocal fluorescence microscopy. In this case, the entire population showed a good uptake of **1**, with no evidence of toxicity, as the cell population evidently maintained a healthy membrane potential, concentrating cationic complex **1** on the cytostolic side of the limiting plasma membrane, visualised by superimposition of the fluorescence image on a transmitted light image, obtained using Nomarski differential interference contrast optics. Furthermore, localisation in specific organelles was evident (Fig. 4(a)–(c)). These are believed to be mitochondria, since the cationic, lipophilic, thiol-reactive nature of **1** would be expected to lead to high levels being localised in mitochondria. Because the transmembrane potential of the inner mitochondrial membrane[1e] is greater than that of the plasma membrane, electrophoretic uptake through each set of membranes should lead to high concentrations of cationic lipophilic species in the mitochondria, and thiol reactivity should then lead to immobilisation due to reaction with reduced thiols in the mitochondria.

While it seemed likely that **1** was accumulating in mitochondria, in order to prove this, studies were undertaken to show that localisation was in the same organelles as those of a known mitochondrial fluorescent probe. Although **1** had been designed to mimic MitoTracker™ dyes, it would be tautological to use a chloromethyl dye to demonstrate the localisation of another chloromethyl species, so instead, another dye, TMRE, lacking this functional group but known to accumulate in mitochondria,[9] was chosen. The patterns of localisation (Fig. 5(a)–(c)) seen with TMRE and **1** under the same incubation conditions were essentially identical, with Fig. 4(a) and Fig. 5(a) illustrating the 'grainy' nature of the organelles, and Fig. 4(b)/(c) and Fig. 5(b)/(c) the similar locality within the membrane, but in the periphery of the cytosol. Finally, co-localisation experiments were attempted, in which **1** and TMRE were incubated with the same cells in order to demonstrate that they were localising in the same organelles. As the emission wavelengths of TMRE and **1** are very close (588 and 551 nm, respectively), it was not possible to distinguish the patterns of localisation of each fluorophore from the emission characteristics, and instead the different excitation maxima (555 and 364 nm, respectively) were utilised to allow the localisation patterns of each fluorophore to be determined.

Using 405 nm laser excitation, only emission from **1** was observed, whereas using 543 nm excitation, only emission from TMRE was observed, and thus the large difference in Stokes shift between these fluorophores, which emit essentially indistinguishable light, allowed the differentiation of their localisation. While it is trivial to demonstrate *in vitro* that **1** (or its thiol derivatives) will not display significant emission when excited at 543 nm, and that, conversely, TMRE will not emit when excited at 405 nm, it would only be by the observation of minor differences in the pattern of localisation for each fluorophore that this differential excitation technique could be validated. While it is impractical to demonstrate exactly the nature of the species present in the mitochondria, the observed luminescence is compatible with that of the glutathione adduct **7** (although **1** and all its derivatives have similar photophysical properties). Observation of the fluorescence patterns in the population treated with both **1** and TMRE showed that the pattern of emission observed from exciting at both wavelengths was essentially identical (Fig. 6 and Fig. 7), indicating either that co-localisation had occurred

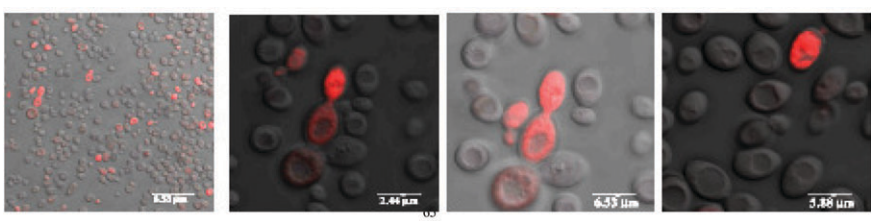


**Fig. 3** Confocal fluorescence microscopy images of **1** incubated with yeast cells.

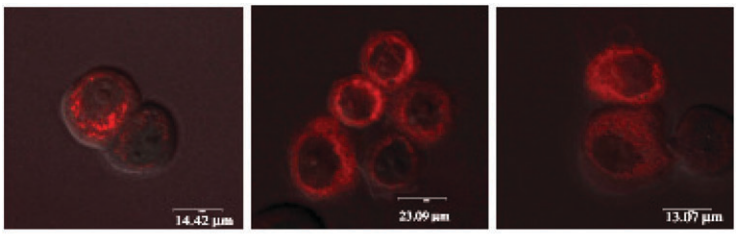


a b c

**Fig. 4** Confocal fluorescence microscopy images of **1** incubated with MCF-7 cells.

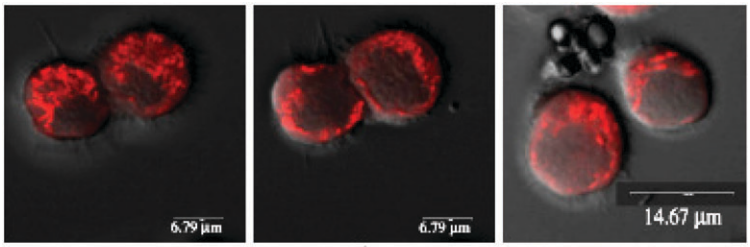


a b c

**Fig. 5** Confocal fluorescence microscopy images of TMRE incubated with MCF-7 cells.



or that the technique was flawed and could not distinguish between the two fluorophores.

Careful examination of the images, however, identified a few cells in which preferential uptake of **1** had occurred. In these cases, excitation at 405 nm led to fluorescence, while excitation at 543 nm did not (Fig. 8). These figures are shown with no transmitted light image for clarity, and with the observed emission obtained at the different excitation wavelengths illustrated in blue for 405 nm and red for 543 nm, combined with an overlayed image. Thus, in the overlayed image, red or blue indicate non-coincidence of localisation and pink or purple indicate co-localisation. Except for a single cell in Fig. 8, all the cells studied showed predominantly pink-to-purple overlays, and the cross-sections of intensity (see, *e.g.*, Fig. 7(c)) showed good agreement with this visual inspection. While no statistical pixel analysis was undertaken (scatter plots are included in the ESI†), it is beyond reasonable doubt that the images obtained are characteristic of the co-localisation of **1** and TMRE. They therefore demonstrate that **1** is a mitochondrion-selective $^3$MLCT rhenium dye, a $^3$MLCT complex that is designed for a specific biological target, and one that may have a promising future for $^3$MLCT biological imaging agents.

We thank the EPSRC National Mass Spectrometry Service Centre, Swansea for mass spectra of the labile rhenium carbonyl complexes and the EPSRC LSI (EP/D080401/1) for financial support.

## Experimental

### General

All starting materials, reagents and solvents were purchased from commercial suppliers and used as supplied, unless otherwise stated. NMR spectra were recorded on a Bruker DPX 400 at 400 MHz for proton and 60 MHz for carbon, unless otherwise reported. IR spectra were recorded on a Perkin-Elmer 1600 FT IR as thin films or Nujol mulls, and are reported in wavenumbers. Mass spectra were recorded on a VG Fisons Platform II instrument or at the EPSRC National Mass Spectrometry Service in Swansea (HRMS). Elemental analyses were performed by Warwick Analytical Services. All photophysical data were obtained on a HORIBA Jobin Yvon Fluorolog spectrometer fitted with a JY TBX picosecond photodetection module and a Hamamatsu R5509-73 detector (cooled to −80 °C using a C9940 housing). The pulsed laser

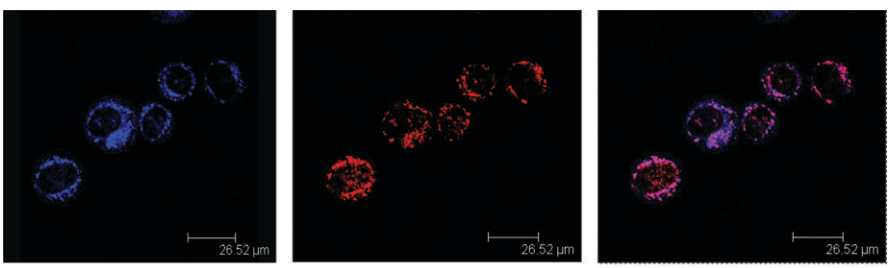


a b c

**Fig. 6** Co-localisation of **1** and TMRE in MCF-7: (a) exciting at 405, (b) exciting at 543, (c) superimposed.

 

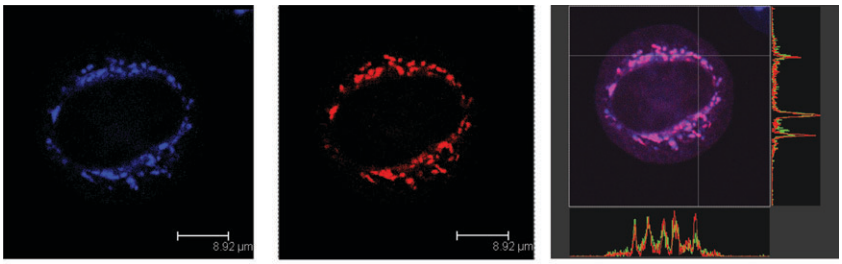


**Fig. 7** Colocalisation of **1** and TMRE in MCF-7 close up and cross section.

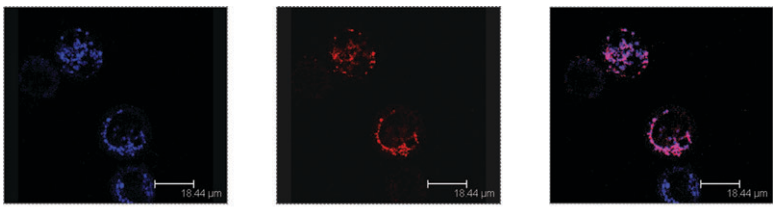


**Fig. 8** Colocalisation of **1** and TMRE in MCF7 showing single uptake in one (bottom) cell.



source was a Continuum Minilite Nd:YAG configured for 355 nm output. Lifetimes were obtained using a HORIBA Jobin Yvon FluoroHub single photon counting module. Solvents were purified according to ref. 10. **4** was prepared according to ref. 4*a*.

### Cell culture and imaging

**Yeast cell incubation with 1.** *Saccharomyces cerevisiae* IFO 0233 cells were harvested by centrifugation (1000 g, 3 min), washed twice in phosphate buffer saline (PBS, pH 7.4), before being resuspended in PBS, incubated with **1** (final concentration 100 μg $ml^{-1}$) for 30 min in 0.3% yeast extract, 1% peptone and 1% glucose, rinsed in PBS (X3) and mounted on a slide. Preparations were viewed using a Leica TCS SP2 AOBS confocal scanning laser microscope using a ×63 or ×100 objective, with excitation at 405 nm and detection at 520–570 nm.

**Human cell incubation with 1.** Human mammary adenocarcinoma cells (MCF-7),[8] obtained from the European Collection of Cell Cultures, Porton Down, Wiltshire, UK, were maintained as adherent cultures in Eagle's Minimum Essential Medium (EMEM) supplemented with 10% foetal bovine serum, penicillin and streptomycin. Cells were detached from the plastic flask using trypsin and EDTA, and were suspended in an excess volume of growth medium. While suspended in this medium, cells were incubated with **1** (final concentration 100 μg $ml^{-1}$) over ice for 30 min. Cells were then washed three times in PBS, harvested by centrifugation (3 min, 800 g), mounted on a slide and viewed as above by confocal microscopy.

**Human cell incubation with TMRE.** MCF-7 adenocarcinoma cells were harvested as indicated above, resuspended in EMEM culture medium and incubated with TMRE (final concentration 20 nM) for 2 h at room temperature, before being washed three times in PBS, mounted and viewed as above by confocal microscopy.

**Co-localisation experiments.** MCF-7 adenocarcinoma cells were harvested as indicated above, resuspended in EMEM culture medium and incubated with both TMRE (final concentration 100 nM) and **1** (final concentration 20 μg $ml^{-1}$) for 1.5 h at room temperature, before being washed three times in PBS, mounted and viewed as above by confocal microscopy. Images were recorded in each case with excitation at either 405 or 543 nm and detection between 500–600 nm.

### *fac*-[Re(bpy)(CO)$_3$PyCH$_2$Cl](PF$_6$) (1)

A solution of *fac*-[Re(bpy)(CO)$_3$PyCH$_2$OH](BF$_4$)[4a] (150 mg, 0.2 mmol) in 3 ml of thionyl chloride was stirred under a nitrogen atmosphere overnight. The mixture was cooled in an ice bath and a saturated aqueous $NH_4PF_6$ solution was added very slowly, dropwise, with extremely rapid stirring until a yellow solid precipitate formed. The precipitate was separated from the mixture of solvents by filtration and washed several times with water to give **1** as a yellow solid (132 mg, 78.3% yield), m.p. 180 °C. $\delta_H$ ($CD_3CN$) 4.58 (2H, s, C$H_2$), 7.33 (1H, m, Py*H*5), 7.82 (2H, m, bpy*H*5,5′), 7.91 (1H, d, $J$ = 4.5 Hz, Py*H*4), 8.20 (1H, d, $J$ = 5.5 Hz, Py*H*6), 8.32 (3H, m, Py*H*2 and bpy*H*4,4′), 8.42 (2H, d, $J$ = 6.4 Hz, bpy*H*3,3′) and 9.18 (2H, d, $J$ = 5.4 Hz, bpy*H*6,6′). $\delta_C$ ($CD_3CN$) 41.1 ($CH_2$), 124.2 (2C(5,5′), bipy), 126.1 (1C(5), py), 128.3 (2C(3,3′), bipy), 136.6 (1C(3), py), 139.0 (1C(4), py), 140.7 (2C(4,4′), bipy), 151.0, 151.1 (1C(2), py, 1C(6), py), 153.4 (2C(6,6′), bipy), 155.2 (2C(2,2′), bipy), 191.2 (1C, $CO_{apical}$) and 195.0 (2C, $CO_{equatorial}$). $\nu_{max}$ (Nujol): 2027s, 1922sb and 1895sb (CO). $m/z$ (ESI) 553.9 $[MH]^+$ and 427.0 $[M - PF_6 - PyCH_2Cl]^+$. Theoretical isotope pattern 552.0 (52%), 553.0 (11%), 554.0 (100%), 550.0 (22%), 556.0 (31%) and 557.0 (8%); observed

isotope pattern 551.9 (50%), 552.9 (11%), 553.9 (100%), 554.9 (22%), 556.0 (30%) and 557.0 (5%). HRMS (ESI) calculated $[M - PF_6]^+$ = 552.0248; measured $[M - PF_6]^+$ = 552.0252. $ReC_{19}H_{14}O_3N_3ClPF_6$ requires C, 32.65; H, 2.02; N, 6.01; found C, 32.46; H, 1.92; N, 5.93%.

### *fac*-[Re(bpy)(CO)$_3$PyCH$_2$SCH$_2$CH(NH$_2$)COOMe](PF$_6$) (6)

L-Cystine methyl ester (59 mg, 0.4 mmol) was added to a de-gassed solution of **1** (50 mg, 0.07 mmol) and triethylamine (0.04 ml, 0.3 mmol) in 10 ml of acetonitrile. After stirring for 1 h under a flow of nitrogen, the solvent was removed and the dark solid remaining was washed with water (2 × 2 ml) to afford **6** as a dark yellow solid (44 mg, 65.4% yield), m.p. 185 °C. $\delta_H$ ($CD_3CN$) 2.22–2.39 (2H, m, C*H*$_2$(Cys)), 3.39 (1H, m, C*H*), 3.50 (2H, s, C*H*2), 7.18 (1H, m, Py*H*5), 7.70–7.75 (3H, m, Py*H*5 and bpy*H*5,5′), 8.03 (1H, d, $J$ = 5.5 Hz, Py*H*6), 8.09 (1H, s, Py*H*2), 8.19 (2H, m, bpy*H*4,4′), 8.28 (2H, d, $J$ = 8.1 Hz, bpy*H*3,3′) and 9.16 (2H, d, $J$ = 5.3 Hz, bpy*H*6,6′). $\delta_C$ ($CD_3CN$) 32.0 ($CH_2$(Cys)), 35.2 ($CH_2$), 51.5 ($CH_3$), 54.2 (CH), 124.5 (2C(5,5′), bipy), 126.2 (1C(5), py), 128.7 (2C(3,3′), bipy), 138.0 (1C(3), py), 140.1 (1C(4), py), 141.0 (2C(4,4′), bipy), 150.3 (1C(6), py), 151.6 (1C(2), py), 153.8 (2C(6,6′), bipy), 155.6 (2C(2,2′), bipy), 192.3 (1C, $CO_{apical}$) and 195.3 (2C, $CO_{equatorial}$). $\nu_{max}$ ($CH_3CN$): 2036s and 1931sb (CO). $m/z$ (ESI) 653.1 $[MH]^+$ and 427.0 $[M - PF_6 - PyCH_2SCH_2CH(NH_2)COOMe]^+$. Theoretical isotope pattern 651.1 (55%), 652.1 (18%), 653.1 (100%), 654.1 (29%) and 655.1 (10%), observed isotope pattern 651.1 (58%), 652.1 (16%), 653.1 (100%), 654.1 (27%) and 655.1 (9%). HRMS (ESI) calculated $[M - PF_6]^+$ = 653.0863; measured $[M - PF_6]^+$ = 653.0868.

### *fac*-[Re(bpy)(CO)$_3$Py-3-CH$_2$SCH$_2$CH[NHCO(CH$_2$)$_2$CH(NH$_2$)COOH]CONHCH$_2$COO$^-$] (7)

L-Glutathione (44 mg, 0.14 mmol) was added to a yellow suspension of **1** (50 mg, 0.07 mmol), and triethylamine (0.04 ml, 0.28 mmol) introduced in 15 ml of de-gassed methanol. Next, 3 ml of de-gassed water was added to the suspension, affording a dark solution, from which a dark precipitate appeared after few minutes of stirring at 40 °C. The mixture of solvents was removed under vacuum and the dark solid remaining was dissolved in water, from which the impurities were filtered off. It was then dissolved in the smallest possible volume of water and passed through an ion exchange column (Amberlite IR120 H resin, $NH_4^+$ form) that had previously been washed with aqueous ammonium chloride, eluting with water. The yellow coloured fraction that eluted immediately was collected, evaporated and dried under vacuum to give **7** as a yellow solid (26 mg, 43.7% yield), m.p. 168 °C. $\delta_H$ ($D_2O$) 1.98 (2H, m, C*H*$_2$(11)), 2.23–2.32 (4H, m, C*H*$_2$(6), C*H*$_2$(10)), 3.62 (5H, m, PyC*H*$_2$,CH$_2$(2), CH(12)), 4.10 (1H, m, C*H*(3)), 7.08 (1H, *t*, $J$ = 7.7 Hz, Py*H*5), 7.62–7.69 (3H, m, Py*H*4, bpy*H*5,5′), 8.08–8.10 (4H, m, bpy*H*4,4′, PyH(6,2)), 8.22 (2H, d, $J$ = 8.2 Hz, bpy*H*3,3′) and 9.17 (2H, d, $J$ = 5.5 Hz, bpy*H*6,6′). $\delta_C$ ($D_2O$) 26.4 (1C(10)), 31.6 (1C (11)), 32.0 (1C(3)), 38.9 ($CH_2$(glu)), 43.5 (1C(2)), 52.6 (1C(12)), 54.3 (1C(6)), 124.6 (2C(5,5′), bipy), 126.5 (1C(5), py), 128.7 (2C(3,3′), bipy), 137.6 (1C(3), py), 140.3 (1C(4), py), 141.2 (2C(4,4′), bipy), 150.9 (1C(6), py), 151.7 (1C(2), py)), 153.9 (2C(6, 6′), bipy), 157.0 (2C(2,2′), bipy), 171.6, 174.2, 174.9, 176.4 (4C(2COOH, 2CON), 192.0 (1C, $CO_{apical}$) and 196.0 (2C, $CO_{equatorial}$). $\nu_{max}$ ($CH_3CN$): 2022s, 1915sb and 1897sb (CO). $m/z$ (ESI) 825.1 $[MH]^+$ and 427.0 $[M - PF_6 - PyCH_2SCH_2CH[NHCO(CH_2)_2CH(NH_2)COOH]CONHCH_2COOH]^+$. Theoretical isotope pattern 823.1 (54%), 824.1 (21%), 825.1 (100%), 826.1 (36%) and 827.1 (11%). Actual isotope pattern 823.1 (58%), 824.1 (20%), 825.1 (100%), 826.1 (34%) and 827.1 (12%). HRMS (ESI) calculated $[M - PF_6]^+$ = 823.1319; measured $[M - PF_6]^+$ = 823.1333.

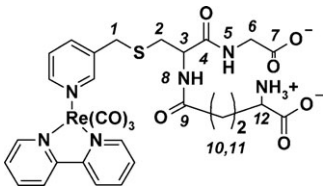


## References


1. (*a*) W. Martin, *Curr. Opin. Microbiol.*, 2005, **8**, 630; (*b*) V. V. Emelyanov, *Eur. J. Biochem.*, 2003, **270**, 1599; (*c*) W. Martin, H. M. McBride, M. Neuspiel and S. Wasiak, *Curr. Biol.*, 2006, **16**, 551; (*d*) C. M. Koehler, K. N. Beverly and E. P. Leverich, *Antioxid. Redox Signaling*, 2006, **8**, 813; (*e*) L. B. Chen, *Annu. Rev. Cell Biol.*, 1988, **4**, 155.
2. A. Macho, D. Decaudin, M. Castedo, T. Hirsch, S. A. Susin, N. Zamzami and G. Kroemer, *Cytometry*, 1996, **25**, 333R. P. Haugland, *A Guide to Fluorescent Probes and Labelling Technologies*, Invitrogen Molecular Probes, Eugene, OR, USA, 10th edn, 2005.
3. M. S. Wrighton and D. L. Morse, *J. Am. Chem. Soc.*, 1974, **96**, 998; M. S. Wrighton, *J. Am. Chem. Soc.*, 1979, **101**, 1597; L. Sacksteder, M. Lee, J. N. Demas and B. A. DeGraff, *J. Am. Chem. Soc.*, 1993, **115**, 8230; D. J. Stufkens and A. Vlcek, Jr, *Coord. Chem. Rev.*, 1998, **177**, 127; K. K.-W. Lo, D. C. Ng, W. Hui and K. Cheung, *J. Chem. Soc., Dalton Trans.*, 2001, 2634.
4. (*a*) A. J. Amoroso, M. P. Coogan, J. E. Dunne, V. Fernández-Moreira, J. B. Hess, A. J. Hayes, D. Lloyd, C. Millet, S. J. A. Pope and C. Williams, *Chem. Commun.*, 2007, 3066; (*b*) K. K.-W. Lo, M. Louie, K. Sze and J. Lau, *Inorg. Chem.*, 2008, **47**, 602.
5. (*a*) S. James, K. P. Maresca, J. W. Babich, J. F. Valliant, L. Doering and J. Zubieta, *Bioconjugate Chem.*, 2006, **17**, 590; (*b*) K. A. Stephenson, S. R. Banerjee, T. Besenger, O. O. Sogbein, M. K. Levadala, N. McFarlane, J. A. Lemon, D. R. Boreham, K. P. Maresca, J. D. Brennan, J. W. Babich, J. Zubieta and J. F. Valliant, *J. Am. Chem. Soc.*, 2004, **126**, 8598; (*c*) J. D. Dattelbaum, O. O. Abugo and J. R. Lakowicz, *Bioconjugate Chem.*, 2000, **11**, 533; (*d*) F. N. Castellano, J. D. Dattelbaum and J. R. Lakowicz, *Anal. Biochem.*, 1998, **255**, 165; (*e*) K. K.-W. Lo, W.-K. Hui, D. C.-M. Ng and K.-K. Cheung, *Inorg. Chem.*, 2002, **41**, 40.
6. B. J. Coe, N. R. M. Curati, E. C. Fitzgerald, S. J. Coles, P. N. Horton, M. E. Light and M. B. Hursthouse, *Organometallics*, 2007, **26**, 2318.
7. D. H. Northcote and R. W. Horne, *Biochem. J.*, 1952, 232.
8. H. D. Soule, J. Vazquez, A. Long, S. Albert and M. Brennan, *J. Natl. Cancer Inst.*, 1973, **51**, 1409.
9. J. E. Whitaker, P. L. Moore, R. P. Haugland and R. P. Haugland, *Biochem. Biophys. Res. Commun.*, 1991, **175**, 387; J. C. Smith, *Biochim. Biophys. Acta*, 1990, **1016**, 1; M. A. Aon, S. Cortassa, K. M. Lemar, A. J. Hayes and D. Lloyd, *FEBS Lett.*, 2007, **581**, 8.
10. D. D. Perrin and W. L. F. Armarego, *Purification of Laboratory Chemicals*, Butterworth-Heinemann, Oxford, 4th edn., 1996.


 